Proceedings World Geothermal Congress 2020+1
Reykjavik, Iceland, April - October 2021

Geophysical Characterization of the Eburru Geothermal Field, Kenya from the Analysis and Interpretation of Magnetotelluric and Gravity Techniques.

Justus. Maithya[1] and Yasuhiro. Fujimitsu[2]

[1]School of Physical Sciences, Department of Physics, Jomo Kenyatta University of Agriculture and Technology (JKUAT), 62000 Kenya.

[2]Faculty of Engineering, Department of Earth Resources Engineering, Kyushu University, Fukuoka, 819-0395 Japan

[1]Corresponding author: *jmmaithya@jkuat.ac.ke*

Keywords: Magnetotelluric, Gravity, 3-D Inversion, Eburru Geothermal Field

ABSTRACT

Magnetotelluric (MT) and gravity surveys were carried out in the area to delineate the heat source, estimate the geothermal reservoir, and assess the extent of geothermal system. Three-dimensional magnetotelluric interpretation of geothermal systems is a powerful tool for characterization of the deep electrical resistivity structure of geothermal reservoirs with high resolution and accuracy. Three-dimensional magnetotelluric (MT) inversion of Eburru datasets using ModEM program was performed to obtain the resistivity structure of the field. The preferred electrical resistivity model shows a conductive zone (< 10 Ωm) interpreted as the cap rock within 1 km from the surface overlaying an intermediate resistive layer (~ 35 Ωm) and a deep conductor (< 10 Ωm) extending from sea level to a depth of 2.5 km below sea level. Additionally, the 3-D resistivity model shows pronounced low resistivity regions which trend in the north-south direction, consistent with the local fault strike. A total of 375 gravity data points were used in creating the Bouguer anomaly, using a Bouguer density of 2.27 g/cm^3. Gravity survey results indicate Bouguer anomaly having both high and low amplitude anomalies. Three-dimensional MT inversion based on full impedance tensor and three- dimensional gravity model obtained by inverting Bouguer anomaly imaged similar features. The gravity model shows that the high-density anomaly bodies occur along the fault zones. A relatively low resistivity and a high density body located approximately 1.5 km below sea level may be related to the geothermal reservoir which is likely heated by magmatic fluid emanating from deeper melt sources.

1. INTRODUCTION

The Eburru volcanic complex is located in the Kenyan rift and is known to have the highest peak in the rift valley with elevation of about 2800 m. It belongs to a complex of volcanoes Menengai, Eburru, Olkaria, Longonot and Suswa that form the Kenya Dome (Figure 1). These volcanoes are prime targets for exploration and geothermal energy production. Thermal expression at the surface in the field is shown by fumaroles, hot spring, and hot and thermally altered grounds. Most of these manifestations are closely associated with the local fault system within a zone of intense fracturing to the south of the field. Deep drilling of six wells to an average depth of 2500 m was done between 1989 and 1991 and currently the field produces 2.5 MW_e utilizing steam from well EW-01. The temperature of the field varies from about 140.1 °C and exceeding 280 °C as observed from the downhole temperature measurements.

All geophysical inversion methods are fraught with the problem of non-uniqueness (e.g., Menke, 1989; Munoz & Rath, 2006). Data acquired in a geophysical survey is usually restricted to the surface of the Earth or the shallow subsurface, often with relatively large spacing between measurement sites, and affected by noise. In such a situation different models can explain the observed data, creating ambiguity in their interpretation (Tarantola, 2004).

The two geophysical methods provide a description of the geological structure with different parameters, resistivity and density. These parameters should describe the same earth but their sensitivity to different processes vary from one another. Magnetotelluric loses resolution with depth but describes well the lateral changes in the structures. Gravity inversion is non-unique but it is intrinsically 3D and allows for horizontal resolution. It needs a priori information to control its intrinsic non-uniqueness. The use of MT method provides information about rock properties, temperature, and the degree of hydrothermal alteration. This information can be used to determine the geometry and depth of the hydrothermal reservoirs, location of fracture zones, and the permeability distribution (Malin et al., 2004). Therefore, understanding the nature of low resistivity zones is fundamental for accurate targeting of high temperature up flow zones. Gravity survey methods are useful in detecting underground fault system. Fault system information can be used to analyze and understand ground water channels and water flow directions. Gravity data may be used to interpret the subsurface, determine the geothermal reservoir and aid in locating prospective heat sources. Integrating the MT and gravity data reduces the intrinsic ambiguity of either dataset and produces a more robust interpretation.

2. GEOLOGICAL SETTINGS

The Eburru volcano forms the highest topography within the entire Kenyan rift at an elevation of about 2800 m. The volcano consists of east and west volcanic centres which are composed of rhyolites, pyroclastics, trachytes, basalts, tuffs and pumice (Lagat, 2003). The two volcanic centres are arranged in an E-W trend and extend as far to the west as the Mau escarpment. The structure of the Eburru field is dominated by faults and fractures that trend in N-S direction (Figure 2). Large open fractures and faults are common on the eastern Eburru volcano forming micro-grabens through the geothermal field. These faults serve as conduits for the geothermal fluids ascent as shown by the abundance of surface manifestations in the form of fumaroles, hot and steaming grounds (Beltran, 2003; Muchemi, 1990; Omenda & Karingithi, 1993; Velador et al., 2003). The faults also act as permeable channels at depth implying that they control the fluid movement. Pyroclastics are widely spread in the field covering western Eburru which has thick vegetation making it difficult for conducting any geophysical surveys (Figure 2). The Badland basalts in the north are of recent age and are not covered by any vegetation. The flows to the south are mainly comendites, rhyolites, trachytes and minor basalts (Simiyu, 1990).

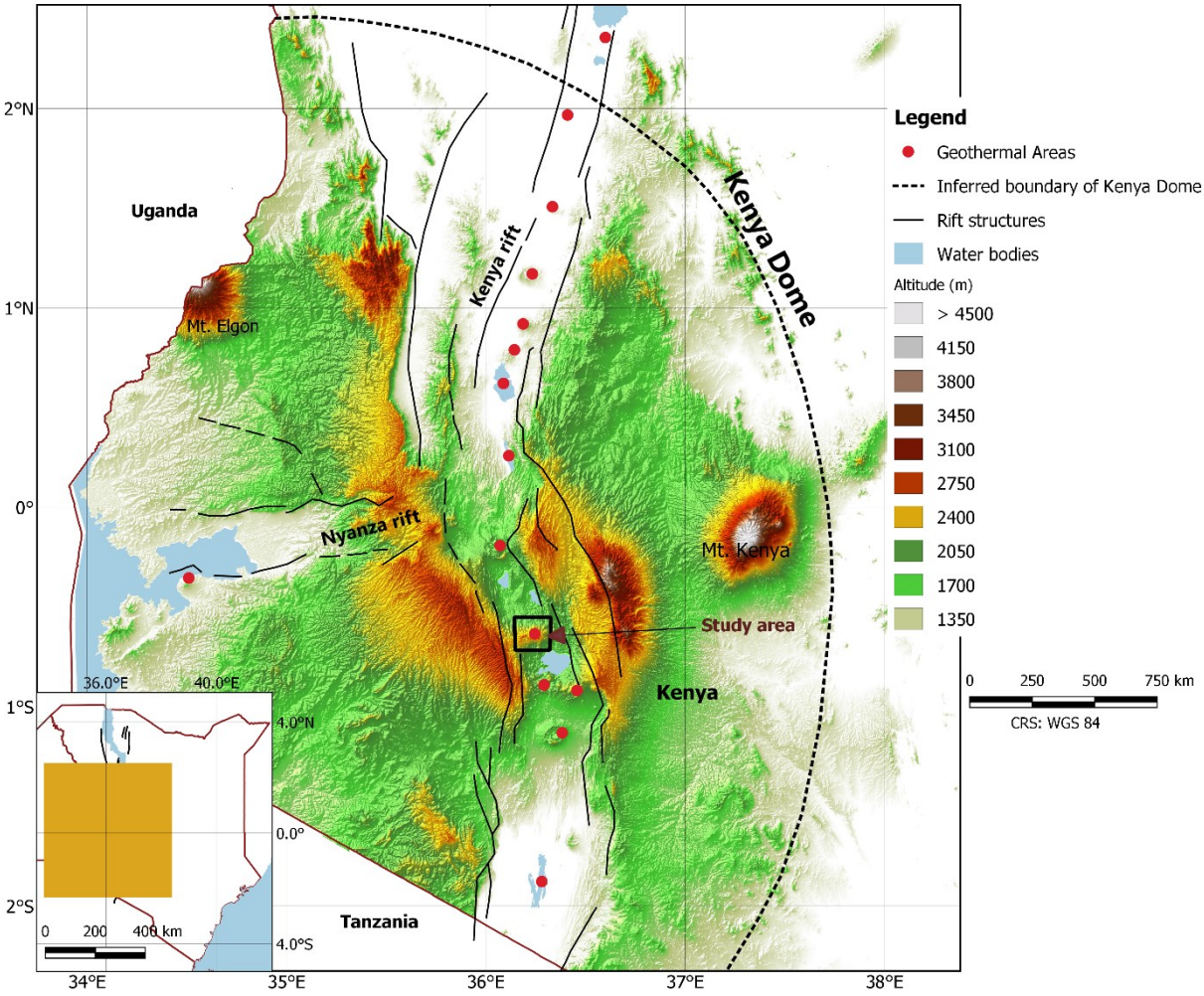

Figure 1: Location Map of the Study Area. The High Altitude (>1500 M Above Sea Level) Area Shows Part of The Kenya Dome.

3. MAGNETOTELLURIC METHOD

Magnetotelluric is a passive electromagnetic method used to investigate the electrical conductivity of the ground (Chave & Jones, 2012). It makes use of the horizontal time varying natural electric $(\mathbf{E})$ and magnetic $(\mathbf{H})$ fields in orthogonal directions on the earth's surface. The complex impedance tensor $(\mathbf{Z})$ describes the relationship between the magnetic and electric fields. This relationship can be expressed mathematically as $\mathbf{E} = \mathbf{ZH}$ or in matrix form as:

$$\begin{pmatrix} E_x \\ E_y \end{pmatrix} = \begin{pmatrix} Z_{xx} & Z_{xy} \\ Z_{yx} & Z_{yy} \end{pmatrix} \begin{pmatrix} H_x \\ H_y \end{pmatrix} \quad (1)$$

$\mathbf{Z}$ contains all the information about subsurface resistivity structure. At a given period, the apparent resistivity is the resistivity equivalent to that of a homogeneous subsurface. In this case the penetration depth can be estimated by the skin depth which increases with subsurface resistivity and period. In 1-D Earth, the diagonal components $\mathbf{Z}$ of will be zero and the off-diagonal components will be equal but opposite in sign. In a 2-D Earth, where $\mathbf{H}$ and $\mathbf{E}$ are parallel and perpendicular to geoelectric strike, the diagonal components of $\mathbf{Z}$ will remain zero while the off-diagonal components will decompose into the transverse magnetic (TM) and the transverse electric (TE) modes. In a 3-D Earth, all components of $\mathbf{Z}$ will be nonzero and the phase tensors will be ellipses elongated in a slewed direction of current flow (Booker, 2014).

The Tipper (T) is complex-valued and frequency dependent like the impedance $\mathbf{Z}$ and describes the relationship between the horizontal $(\mathrm{H_x}$ and $\mathrm{H_y})$ and the vertical $(\mathrm{H_z})$ magnetic fields, i.e.

$$\mathrm{H_z} = \mathrm{T_{zx}H_x} + \mathrm{T_{zy}H_y} \quad (2)$$

3.1 Magnetotelluric Survey

This study used a total of 107 soundings collected by a team from Kenya Electricity Generating Company (KenGen) in 2006, 2013 and 2016. The MT data were acquired with phoenix MTU-5A recording instruments using porous pot electrodes and three induction

coils which have the ability to detect changes in resistivity to great depths. The electrodes are used to determine the electric field which is derived from voltage difference electrode pairs E_x and E_y while the induction coils measure the magnetic fields H_x, H_y and H_z in three orthogonal directions. The distance between the electrodes was approximately 60 m depending on the terrain. The ratio of the recorded magnetic and electric fields gives an estimate of the apparent resistivity of the ground at any given depth. Instruments recorded for an average of 18 hours so as to collect data for long periods and also take advantage of the strong signals usually available in the late hours of the night hence get good sampling of the MT response. A remote reference site was based in Olkaria 30 km from Eburru field a place thought of to be geologically stable and with minimum noise influence in order to remove electromagnetic noise from the electromagnetic signals at each measuring station. The MT time series were processed using the programs SSMT2000 and MT editor (Phoenix Geophysics, 2005) to produce cross-power estimates and generate EDI files (Wight, 1991).

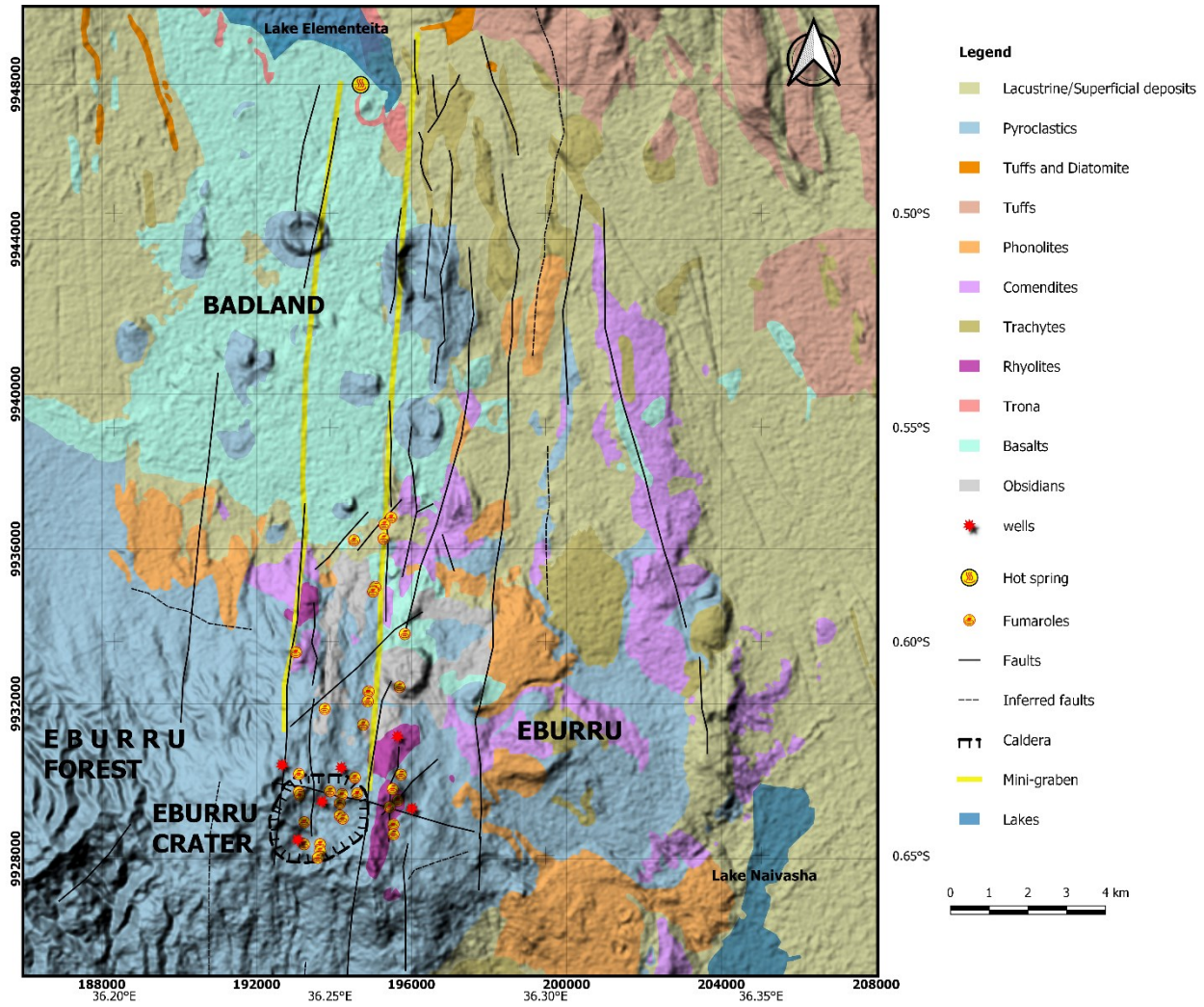

Figure 2: Geological Map of The Eburru Geothermal Field (Modified from Thompson & Dodson, 1963).

3.2. Data Analysis

Dimensionality of the MT response can give an indication of complexity of the subsurface resistivity structure and prescribe the number of model dimensions needed (Martí, 2014). The dimensionality of the data was determined using phase tensor (Caldwell et al., 2004). The results from dimensionality analysis shows 1-D and 2-D features at shallow depth and 3-D features at deeper depth. Therefore, to image deep resistivity structure there was need to carry out three-dimensional MT inversion.

A distortion removal technique was applied to the soundings which appeared to have suffered some degree of distortion following the method by Bibby et al. (2005). The static shift problem of the tensors due to local topography were corrected using a spatial median filter method with a diameter of 3 km applied to sites which exhibited a significant split of apparent resistivity mainly at high frequencies. The curves on the left side of Figures 3 and 4 shows the raw data collected while those on the right side displays the results after the distortion and static shift removal. Period acts as a proxy for depth, with short periods sensing shallow structures and long periods sensing deeper structures. To accommodate any remaining static shifts that had not been addressed by the median method, an apparent resistivity error floor of 5 % was used. In addition, ModEM programme is designed such that it introduces a scattered conductivity distribution in the near-surface layers hence being able to account for any remaining static shift effects (Meqbel et al., 2014; Tietze & Ritter, 2013).

3.3 MT Three-dimensional Modeling

MT data was inverted to produce a preferred 3-D electrical resistivity model using ModEM (Egbert & Kelbert, 2012; Kelbert et al., 2014; Meqbel, 2009) inversion program that utilizes a nonlinear conjugate gradient method. The initial model is updated iteratively

by line search strategy. The 3-D forward problem is based on the finite difference method (FDM). The 3-D inversion was applied to 107 MT soundings and we constructed a model consisting 80, 53 and 50 cells in the x, y and z directions respectively, including x padding of 5 and y padding of 4. The cell dimension in the x and y directions were set at 400 m each and in the vertical direction, a total of 50 layers were used with a first layer thickness of 10 metres increasing for the subsequent layers with a factor of 1.1. The full impedance tensor was inverted in the frequency range of 0.00034 Hz to 319.49 Hz for a total of 80 frequencies. The starting model was a homogeneous half space of 50 Ωm. The starting RMS at the start of the inversion was 32.38, and decreased to 4.49 after 132 iterations (Maithya & Fujimitsu, 2019). The data misfit of the final model was satisfactorily as observed from most of the soundings (Figure 5).

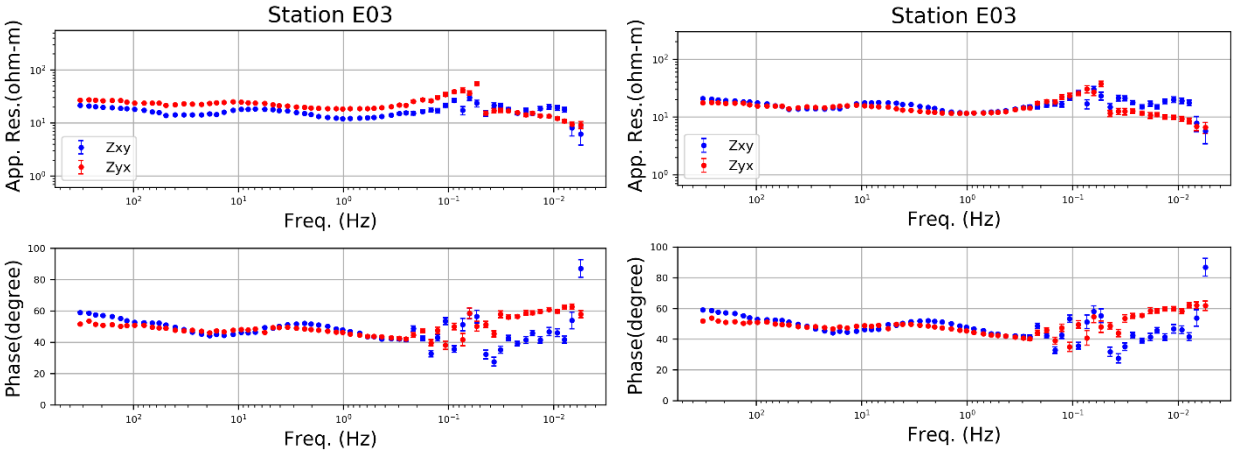

Figure 3: Typical Magnetotelluric Data Collected in the Study Area Displayed as Apparent Resistivity and Phase Curves for Site E03.

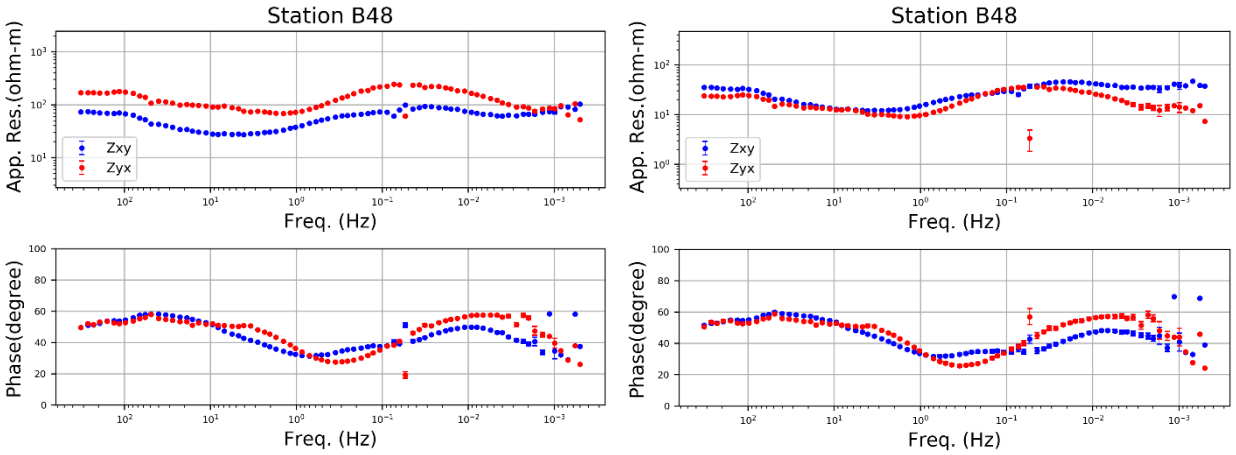

Figure 4: Typical Magnetotelluric Data Collected in the Study Area Displayed as Apparent Resistivity and Phase Curves for Site B48.

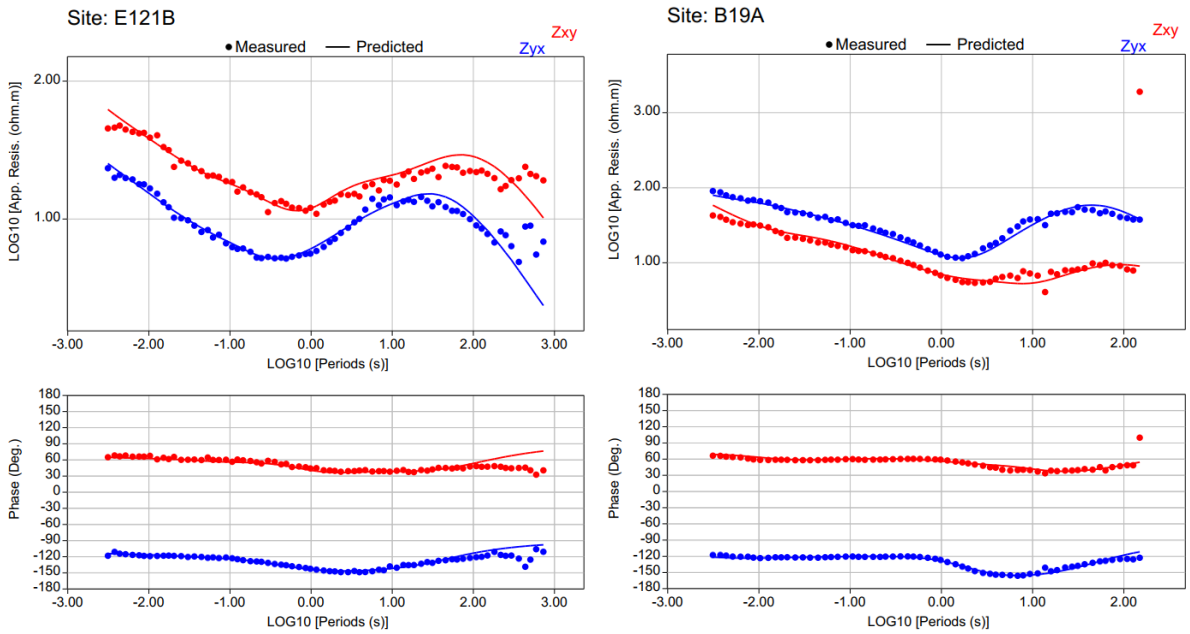

Figure 5: Data Misfit between the Observed and Calculated Apparent Resistivity and Phase Parameters of Zxy (Red Dots) And Zyx (Blue Dots) Components for Station E121 B and B19A. The Dots Represent the Measured Values, and The Line Represents the Calculated Response.

4. GRAVITY METHOD

Gravity is a simple and important passive geophysical technique that yields information on the subsurface density distribution (Blakely, 1996; Nettleton, 1939). It is a potential field technique which measures variations in the Earth's gravitational field. These variations are caused by density contrasts in the near surface rock, sediment and basement rocks. In geothermal exploration, gravity method generally is used to delineate subsurface structures that control the geothermal system. Basically, a given geothermal reservoir and its fluid content cause density differences between the surrounding rocks and the geothermal reservoir.

4.1 Gravity Survey

The gravity dataset used in this study covers an area of approximately 274 km^2 and a total of 375 stations. Gravity survey was carried out by KenGen in Eburru geothermal field in 2016 and 2017. Measurement stations focused on areas in rather flat and with easily accessible terrain settings. Measurements were done at the beginning of the survey of any given day at a designated station (reference station), repeated at the close of the daily survey. The differences obtained were plotted against the time between the two readings at a station in order to correct the drift problem. One of the most important task in gravity data reduction is the choice of the reduction density applied to the terrain and Bouguer corrections. The amplitude and shape of the resulting complete Bouguer anomaly can vary with the reduction density used which directly influences the resulting model. After applying the necessary reductions to the collected data, several mathematical methods were selected and used to obtain a better approximation of Bouguer density. The data set was processed with an average bouguer density of 2.27×10^3 kg m^{-3} obtained from F-H (Parasnis, 1952, 1986) and Comparison with variance of the upward-continuation (CVUR) (Komazawa, 1995) methods and deemed enough to produce a smooth anomaly. A Bouguer gravity map was created, which becomes the basic map for gravity interpretation. Interpretation of Bouguer anomaly was limited to the distribution of survey stations. Areas with no stations were removed and structures located in areas with sparse stations interpreted with caution, nevertheless, the areas considered relevant to this study appear to be well covered during the survey. The complete Bouguer anomaly contains superposition of regional and residual anomalies. The regional Bouguer gravity anomaly results from the presence of broader and deeper structures while the residual Bouguer gravity anomaly is resulting from the presence of smaller and superficial ones. In order to highlight the structures of interest for this study, a regional-residual separation was conducted. A residual gravity anomaly map was created in order to highlight and interpret the anomalies caused by density variation, that could also be related to geological structures in the area. We constructed the residual map using the Generic Mapping Tools (GMT) GRDTREND tool an open source. This tool fits trend surface to grids and computes residuals. A comparison between the residual anomaly map and the geology map shows a close relationship between the two. The residual map shows high gravity values in the southern part of the field where the fumarolic activity takes place and in the northern part where there is existence of a hot spring. The high gravity values are inferred to be faults which are in agreement with the local fault system as mapped from geological studies.

4.2 Gravity Three-dimensional Modeling

3-D gravity modelling of the complete bouguer anomaly was conducted to determine the shape and depth of the geological structures controlling the geothermal system. This was guided by the fact that, the integrated gradient interpretation techniques for edge detection have the ability to detect steep gradients and indicate the location of either faults or geological boundaries but they cannot estimate their depth (Nishijima & Naritomi, 2017). Gravity data Inversion is generally fraught with problems due to data noise and inhomogeneity of geological bodies so even with accurate measurements and correct data reduction one may not obtain geologically reasonable results. To minimize these problems and produce realistic results an addition prior information is required to constrain the model. In this study borehole geology from the six drilled wells was integrated to produce a reasonable source model estimation. The lithostratigraphy is composed of trachytes, pyroclastics, tuffs, obsidian, basalt, rhyolites and syenite. The actual measurements of rock densities of this wells were not available and therefore representative densities were estimated from literature. A density contrast of between -0.28×10^3 kg m^{-3} and 0.55×10^3 kg m^{-3} was obtained by subtracting the Bouguer density from the rock densities for

each of the rock types. The resulting density contrast was gridded to a distance of 50 m which became a reference model or constrain. Results from MT method (Maithya & Fujimitsu, 2019) had shown that the geothermal system was confined on the southern part of the field and this was in agreement with the geology and fumarolic activity. Therefore, gravity inversion was carried out on the same area in order to understand the system and delineate geological structures controlling it. A model consisting of 50, 45 and 45 rectangular cells in the x, y and z-direction, respectively was created. The size of a rectangular cell was set to 250 m and 250 m along respective x and y directions. The height of the cells was set to increase from a top layer of 50 m by a factor of 1.08 for each successive deeper layer.

5. RESULTS

The idea of interpreting the two geophysical methods together was to give a better understanding of the structures controlling the geothermal system in the study area. The local fault system in this geothermal field trend in the north-south direction and therefore cross-sections from both the models would give an insight of the flow of the geothermal fluid in the system. This is due to the fact that faults are likely to act as pathways of fluid ascending from deeper parts to the surface. In order to interpret the structures obtained from both MT and gravity models, a resistivity and gravity profile crossing major geological structures and target the geothermal reservoir area were extracted. Electrical resistivity features C1 and C2 were imaged in the resistivity model trending from west to east of the field. Conductor C1 (~ 5 Ωm) is located directly above conductor C2 (~ 10 Ωm) and they appear to be connected (Figure 6). An intermediate resistive zone (~ 25 Ωm) is found in between the two conductors where well EW-04 is seen to terminate. A high resistive body is observed on the right hand side of the two conductors extending from deeper parts to the near surface.

A cross-section which was extracted from the gravity model images a high dense body > 2.5 g/cm^3 where well EW-04 is observed dipping (Figure 7). This high dense body exists at the same depth as the intermediate resistive zone found in Figure 6. This body overlies a less dense body stretching to deeper region and extending to the eastern side of the field.

6. DISCUSSION

To better interpret the profile resistivity distribution (Figure 6), lithological logs and downhole temperature logs were used in order to obtain a reliable representation of the resistivities from the inversion. The low resistivities observed in the near-surface section is caused inferably by hydrothermal alteration. The resistivity of this layer, commonly known as the smectite zone (mainly in the range of 1-10 Ωm), is usually determined by the type and intensity of alteration process, transformed by the amount of water saturation and temperature (Anderson et al., 2000; Ussher et al., 2000). Conductor C1 is highly conductive found approximately 1000 m in depth which is likely to be dominated by low-temperature alteration minerals was interpreted to be the cap rock (Moore et al., 2008). The clay cap region is very conductive and serve as cover for trapping and keeping heat and hot fluid which are key in the geothermal system (Raharjo et al., 2010). Underlying this region is an intermediate resistive zone where hot fluids ascend from deeper parts through fractured formations or narrow faults increasing its temperature. The low resistive conductor C2 found below C1 could be as a result of magmatic fluid components emanating from deeper melt sources. It is likely to be responsible for heating the intermediate resistive zone interpreted as the propylitic zone (15-60 Ωm) of the system. This zone which is the hotter part of the geothermal system beneath the highly conductive clay cap, interpreted as the heart of the reservoir, is characterized by relatively higher resistivities. The two conductors appear to be connected implying that there exists a fault zone which may be the means for transporting fluid to provide high temperature in the field (Wannamaker et al., 2006). This is in agreement with the local fault system trending in the south-north direction. The occurrence of this conductors is consistent with the formation of fumarolic activity in the south west part of the field. The fumaroles appear to exist along the faults which supports the interpretation that hot fluid use the local fault system to migrate to the surface. The high resistive body found on the right hand side of the two conductors might be due to cold formation. A cold formation/structure would suggest a possible recharge to the geothermal reservoir.

Cumming (2009) and Stimac et al. (2008) proposed a general geothermal resource conceptual model in which they suggested three altered zones which include Smectite zone, Argillic zone, and Propylitic zone (chlorite, epidote, illite, muscovite, biotite). Smectite alteration zone is characterized by the formation of Smectite clay and low to atmospheric temperature alteration minerals. Argillic alteration zone is characterized by the formation of illite and other low to moderate temperature minerals while propylitic alteration zone has high temperature minerals resembling chlorite, biotite, epidote and quartz, with lesser quantities of calcite and albite (Mielke et al., 2015). From the down hole temperature log results, the propylitic zone in the productive wells was encountered at a temperature of 238 °C. This zone coincides with high density body (Figure 7) which is likely to be the geothermal reservoir of the system. There is close relationship between the occurrence of the high-density anomalous structure and the existence of geological faults. Hydrothermal systems can produce either low or high density alteration depending on if the host rock is altered to clay minerals or whether the void space is mineralized by circulating fluids and thereby increasing density (Allis, 1990). Therefore, there is a possibility that the change in density in the area might be caused by large fluid circulation precipitating minerals into void space. The flow of magmatic fluid components along the faults in the shallow parts of the system are likely to have caused the differences in density distribution with depth. The location of hydrothermal activities in most cases describes the zones of high thermal anomalies generally located close to or on the fault structures. This fault structures offer a pathway for fluids to rise to the surface showing zones of hydrothermal upwelling. The fumaroles appear to be located right on top of the dense formation and connected to the fault system.

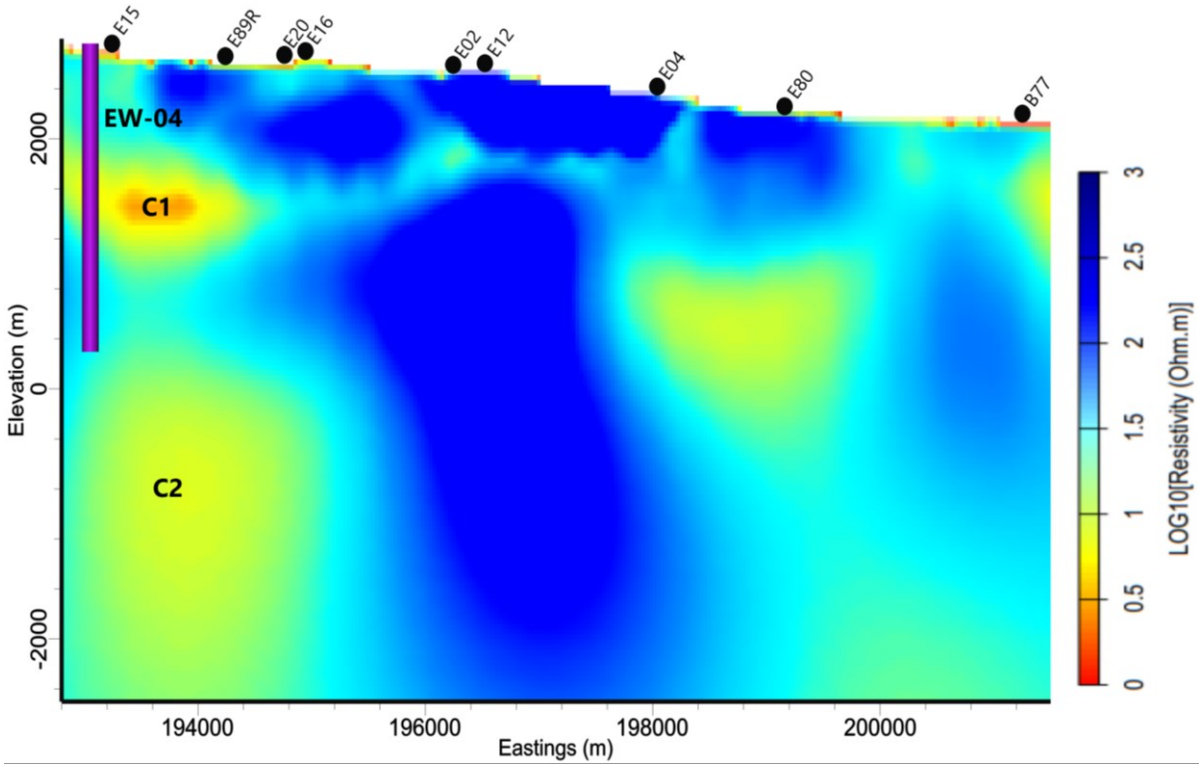

Figure 6: 3-D Resistivity Model

Resistivity and gravity data support a similar interpretation for the two profiles extracted from the three-dimensional models. The two profiles intersect the high-density body hence showing a good relationship between the dense and conductive bodies giving more insights into major subsurface structures governing the geothermal system.

6.1 MT and Gravity joint interpretation

In order to further correlate the resistivity structure and the high dense body, an isosurface of 70 Ωm and a dense body of 2.45 g/cm^3 were obtained from the resistivity and gravity models respectively. The two models were used to show how the high dense body and the intermediate resistive zone relates with the resistive zone.

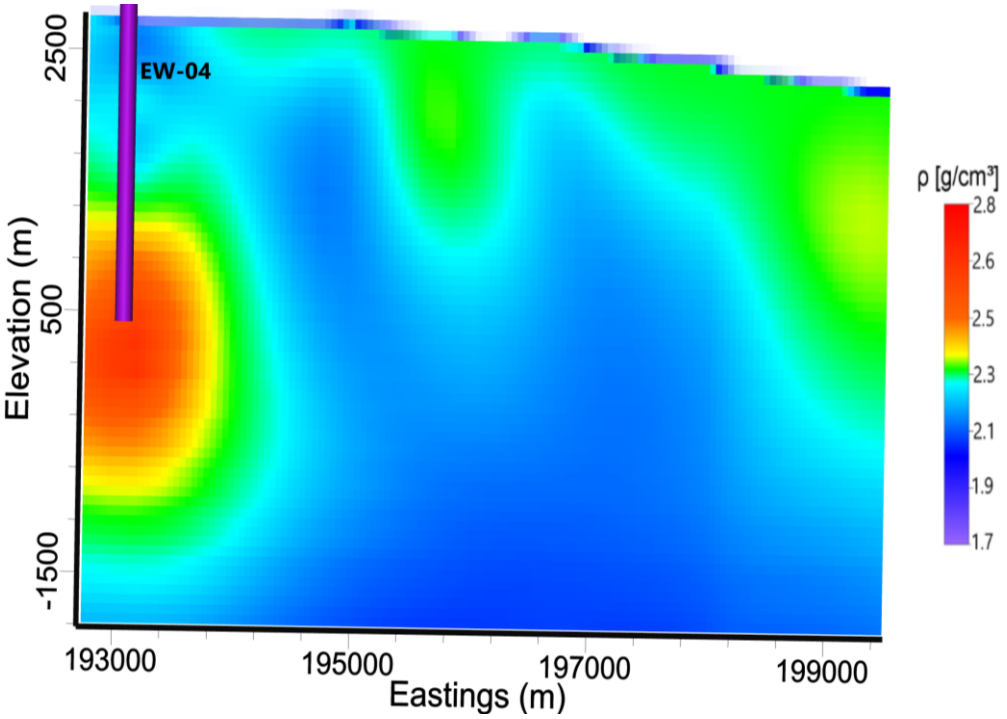

Figure 7: A Cross-section of 3-D Gravity Model

The resistive part appears to mantle the dense body showing that the two have different formation properties as shown in Figure 8. The resistive body could as well be interpreted as cold formation in which the water from the lake Naivasha might have seeped down

through the existing faults possibly recharging the geothermal system. The planar on Figure 8 shows two high density anomalies which appear to enclose a low density anomaly. These high anomalies coincide with the edges of the mini graben while the low density region is covered by pyroclastics. The gravity highs are interpreted as being due to the intrusion of dense magma-derived material into the country rock along fault zones

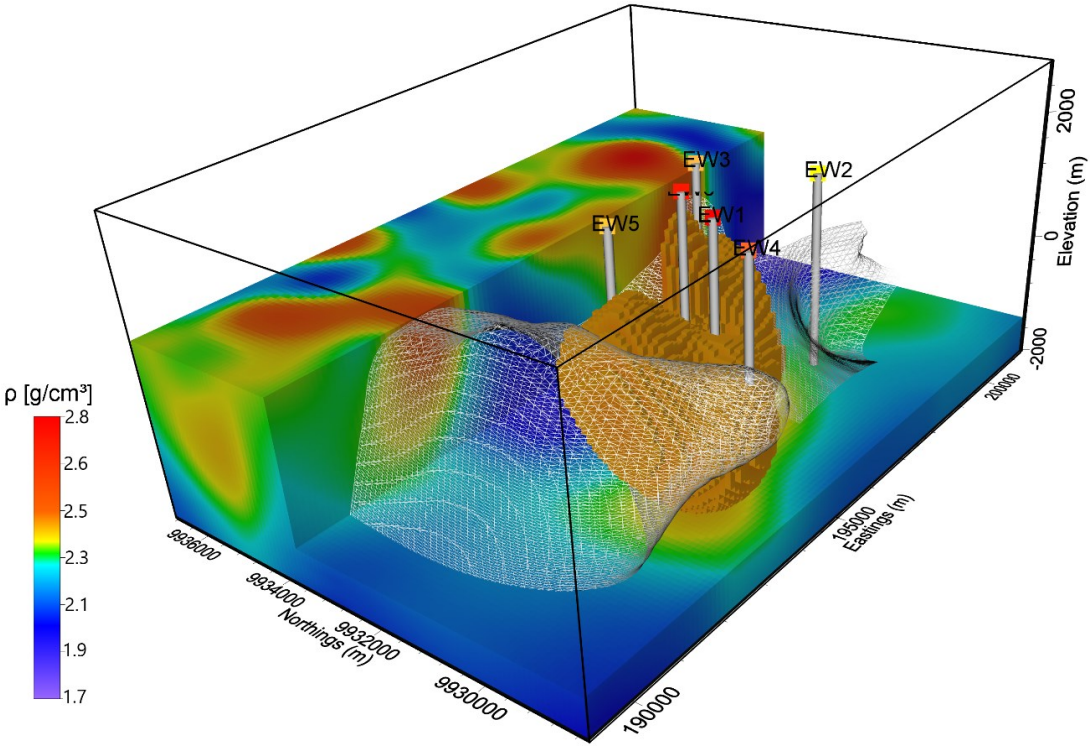

Figure 8: 3D Geometry of the Dense Body (Brown Structure, 2.45 × 10^3 kg m^{-3}) and a Resistive Isosurface (Transparent Mesh, 70 Ωm) The planar View is a Horizontal Slice of Density Anomaly 2000 m bsl.

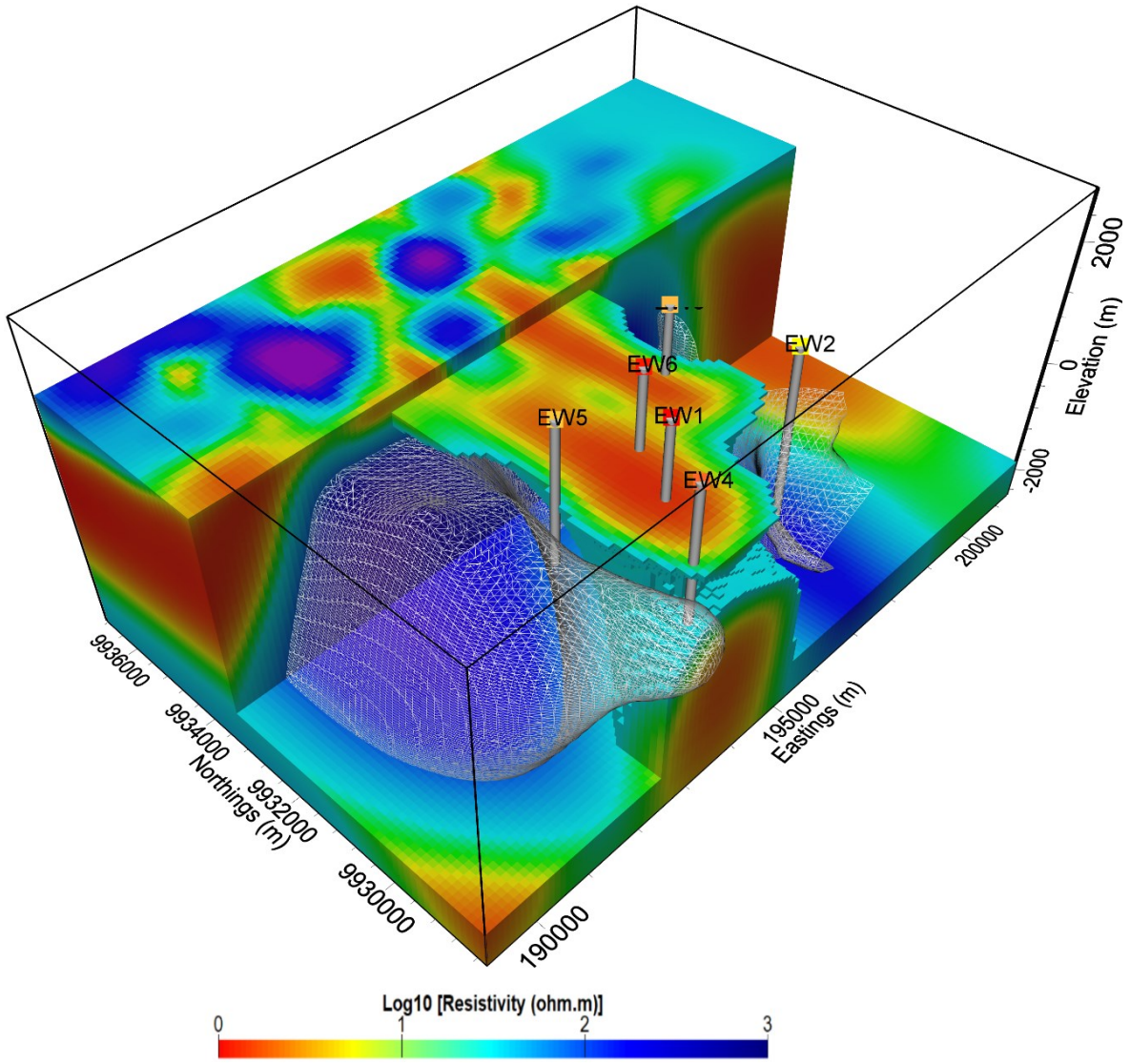

Figure 9: A Perspective Model of 3D Magnetotelluric Inversion. The Model Represents Magnetotelluric Results in Which an Isosurface of 70 Ωm Surrounds a Relatively Less Resistive Body ~30 Ωm. The Planar View is a Resistivity Horizontal Slice at 2000 M B.S.L

The high resistive body in Figure 9 appears to surround the intermediate resistive zone, and this suggests the occurrence of the two structures are interrelated. The intermediate resistive body was interpreted to be the geothermal reservoir which happens to be confined within the caldera while the high resistive structure is likely to be a cold formation. The proposed recharge zone lies within a resistive region which might be caused by cold water movement. The location of this zone also is in line with the assumption that the general flow of fluid from this region is from south to north. Lake Naivasha located on the lower side of this field might be recharging the system hence contributing to the high resistive structure. Such deep fluid movement is likely to occur with the help of geological structures that can allow free fluid motion, and this can be supported by the occurrence of fumarolic activities confined within this region. The presence of fumarolic activities and low resistivity in this region is likely to be associated with the rise of magmatic fluid components beneath the dense body where the heat source is believed to be hosted.

The 3-D gravity inversion images similar structures which were also observed by the 3-D magnetotelluric inversion, hence the results from the two models are in agreement. The reservoir according to MT is associated with an intermediate resistive layer in depth with values between 15 and 60 Ωm, a thickness of 900 – 1100 m. The good correlation between both models gives greater consistency to the structures where the reservoir is associated with a high density body and an intermediate resistive layer which is also confirmed by drilling. For MT, the intermediate resistive region is the propylitic zone where hot geothermal fluids, migrate upwards along fractured formations and narrow faults. This region coincided with a high density anomaly of 2.45 g/cm^3 which represents the hydrothermal alteration zone that hosts the propylitic altered rocks.

7. CONCLUSION

In this work, a joint interpretation of magnetotelluric and gravity models was done. The resistivity profile extracted from the 3-D model shows a conductive zone (< 10 Ωm) interpreted as the cap rock of the system which overlies an intermediate resistive layer (~ 35 Ωm) and a deep conductor (< 10 Ωm) stretching from sea level to a deeper depth. The deeper conductive anomaly may be caused by magmatic fluid components emanating from deeper melt sources. The intermediate resistive layer where the productive wells are seen dipping is likely the geothermal reservoir being heated by the high conductive body beneath it. The profile extracted from the gravity model imaged a high density anomaly body located almost at the same point where the intermediate resistive body appears

to exist. The two geophysical methods used in this work imaged the geothermal reservoir similarly. From the inversion results of gravity and MT data, a clear relationship in the geometry of the dense body relative to the resistive body exists. The joint interpretation enabled us to highlight the structures controlling the geothermal system and better constrain the position and geometry of the geothermal reservoir.

ACKNOWLEDGMENT

The authors of this work would like to thank Japan International Cooperation Agency (JICA) for supporting this research and Kenya Electricity and Generating Company (KenGen) for providing MT data for use in this research. The authors also thank Gary Egbert and Anna Kelbert for providing the ModEM code.

REFERENCES

Allis, R. G. (1990). Geophysical anomalies over epithermal systems. *Journal of Geochemical Exploration*, *36*(1–3), 339–374.

Anderson, E., Crosby, D., & Ussher, G. (2000). Bulls-Eye!—simple resistivity imaging to reliably locate the geothermal reservoir. In *Proceedings of the 2000 World Geothermal Congress, Kyushu–Tohoku, Japan.* (pp. 909–914).

Beltran, J. V. (2003). The origin of pantellerites and the geology of the Eburru volcanic complex, Kenya Rift, Africa.

Bibby, H. M., Caldwell, T. G., & Brown, C. (2005). Determinable and non-determinable parameters of galvanic distortion in magnetotellurics. *Geophysical Journal International*, *163*(3), 915–930.

Blakely, R. J. (1996). *Potential theory in gravity and magnetic applications*. Cambridge University Press.

Booker, J. (2014). The Magnetotelluric Phase Tensor: A Critical Review. *Surveys in Geophysics*, *35*, 7–40.

Caldwell, T., Bibby, H., & Brown, C. (2004). The magnetotelluric phase tensor. *Geophysical Journal International*, *158*(2), 457–469.

Chave, A., & Jones, A. (2012). *The magnetotelluric method: Theory and practice*. Cambridge Universitty Press.

Cumming, W. (2009). Geothermal resource conceptual models using surface exploration data. In *Proceedings, Thirty-Fourth workshop on Geothermal Reservoir Engineering*. Stanford University, Stanford, California.

Egbert, G. D., & Kelbert, A. (2012). Computational recipes for electromagnetic inverse problems. *Geophysical Journal International*, *189*, 251–267.

Kelbert, A., Meqbel, N., Egbert, G. D., & Tandon, K. (2014). ModEM: A modular system for inversion of electromagnetic geophysical data. *Computers and Geosciences*, *66*.

Komazawa, M. (1995). Gravimetric analysis of Aso volcano and its interpretation. *Journal of the Geodetic Society of Japan*, *41*(1), 17–45.

Lagat, J. (2003). Geology and the geothermal systems of the southern segment of the Kenya Rift. *Proceedings of the International Geothermal Conference, Reykjavik.*

Maithya, J., & Fujimitsu, Y. (2019). Analysis and interpretation of magnetotelluric data in characterization of geothermal resource in Eburru geothermal field, Kenya. *Geothermics*, *81*, 12–31.

Malin, P. E., Onacha, S. A., & Shalev, E. (2004). A collaborative joint geophysical imaging project at Krafla and IDDP.

Martí, A. (2014). The Role of Electrical Anisotropy in Magnetotelluric Responses: From Modelling and Dimensionality Analysis to Inversion and Interpretation. *Surveys in Geophysics*, *35*(1).

Menke, W. (1989). *Geophysical data analysis: Discrete inverse theory*. International Geophysics Series, Academic press, San Diego, CA.

Meqbel, N. M., Egbert, G. D., Wannamaker, P. E., Kelbert, A., & Schultz, A. (2014). Deep electrical resistivity structure of the northwestern US derived from 3-D inversion of USArray magnetotelluric data. *Earth and Planetary Science Letters*, *402*, 290–304.

Meqbel, N. M. M. (2009). The electrical conductivity structure of the Dead Sea Basin derived from 2D and 3D inversion of magnetotelluric data. *Ph.D. Thesis*.

Mielke, P., Prieto, A. M., Bignall, G., & Sass, I. (2015). Effect of hydrothermal alteration on rock properties in the Tauhara Geothermal Field, New Zealand. In *World Geothermal Congress* (p. 15).

Moore, J. N., Allis, R. G., Nemčok, M., Powell, T. S., Bruton, C. J., Wannamaker, P. E., … Raharjo, I. (2008). The evolution of volcano-hosted geothermal systems based on deep wells from Karaha–Telaga Bodas, Indonesia. *American Journal of Science*, *308*(1), 1–48.

Muchemi, G. (1990). *Geology of Eburru. Discussion papers for Scientific Review Meeting, Kenya Power Company Limited, internal report.*

Munoz, G., & Rath, V. (2006). Beyond smooth inversion: the use of nullspace projection for the exploration of non-uniqueness in MT. *Geophysical Journal International*, *164*(2), 301–311.

Nettleton, L. L. (1939). Determination of density for reduction of gravimeter observations*. *Geophysics*, *4*(3), 176–183.

Nishijima, J., & Naritomi, K. (2017). Interpretation of gravity data to delineate underground structure in the Beppu geothermal field, central Kyushu, Japan. *Journal of Hydrology: Regional Studies*, *11*, 84–95.

Omenda, P., & Karingithi, C. (1993). Hydrothermal model of Eburru geothermal field, Kenya. Geothermal Resources Council., presented at Short Course III on Exploration for Geothermal Resources, organized by UNU-GTP and KenGen, at Lake Naivasha, Kenya, October 24 - November 17, 2008.

Parasnis, D. S. (1952). A study of rock densities in the English Midlands. *Geophysical Supplements to the Monthly Notices of the Royal Astronomical Society*, *6*(5), 252–271.

Parasnis, D. S. (1986). *Principles of applied geophysics*. Chapman and Hall.

Phoenix Geophysics. (2005). Data Processing User Guide. Phoenix Geophysics Ltd, ON, Canada.

Raharjo, I. B., Maris, V., Wannamaker, P. E., & Chapman, D. (2010). Resistivity structures of Lahendong and Kamojang Geothermal systems revealed from 3-D Magnetotelluric Inversions, a comparative study. In *proceedings world geothemal congress* (p. 6). Bali, Indonesia.

Simiyu, S. M. (1990). *The gravity structure of Eburru, Kenya*. UNU Geothermal Training Programme, Orkustofnun-National Energy Authority, Reykjavik, ICELAND.

Stimac, J., Nordquist, G., Suminar, A., & Sirad-Azwar, L. (2008). An overview of the Awibengkok geothermal system, Indonesia. *Geothermics*, *37*(3), 300–331.

Tarantola, A. (2004). *Inverse problem theory* (1st ed.). SIAM, Philadelphia, PA.

Thompson, A. O., & Dodson, R. G. (1963). *Geology of the Naivasha Area. Geological Survey Kenya, Report No.55, 88p.*

Tietze, K., & Ritter, O. (2013). Three-dimensional magnetotelluric inversion in practice—the electrical conductivity structure of the San Andreas Fault in Central California. *Geophysical Journal International*, *195*(1), 130–147.

Ussher, G., Harvey, C., Johnstone, R., & Anderson, E. (2000). Understanding the resistivities observed in geothermal systems. In *proceedings world geothermal congress* (pp. 1915–1920). Kyushu, Japan.

Velador, J., Omenda, P., & Anthony, E. (2003). An integrated mapping and remote sensing investigation of the structural control for the fumarole location in the Eburru volcanic complex, Kenya rift. Geothermal Resources Council, Transactions, 27. October 12-15.

Wannamaker, P. E., Hasterok, D. P., & Doerner, W. M. (2006). Possible magmatic input to the Dixie Valley geothermal field, and implications for district-scale resource exploration, inferred from magnetotelluric (MT) resistivity surveying. In *Geothermal Resources Council Transactions, 30* (pp. 471–475).

Wight, D. (1991). MT/EMAP Data Interchange Standard: Tulsa, Oklahoma. *Society of Exploration Geophysicists*.